Phase development in the catalytic system V$_2$O$_5$/TiO$_2$ under oxidising conditions

D. Habel [a,*], J.B. Stelzer [c], E. Feike [a], C. Schröder [a], A. Hösch [b], C. Hess [d],
A. Knop-Gericke [d], J. Caro [c], H. Schubert [a]

[a] *Institute for Material Science and Technologies, TU Berlin, Englische Straße 20, D-10587 Berlin, Germany*
[b] *Institute for Applied Geosciences, TU Berlin, Straße des 17. Juni 135, D-10669 Berlin, Germany*
[c] *Institute for Physical Chemistry and Electrochemistry, University of Hanover, Callinstraße 3-3a, D-30167 Hanover, Germany*
[d] *Fritz-Haber-Institute of the Max Planck Society, Department of Inorganic Chemistry, Faradayweg 4-6, D-14195 Berlin, Germany*

Abstract

The target of this work was to investigate phase development in the catalyst system consisting of TiO$_2$ (anatase) and V$_2$O$_5$ (Shcherbinaite). Thus, a set of V$_2$O$_5$/TiO$_2$ specimens was prepared by ball milling and exposed to subsequent annealing in air in the temperature range from 400 to 700 °C. The XRD-results showed the presence of anatase and shcherbinaite as the only phases up to 525 °C. For temperatures above 525 °C the peak intensities were diminishing and rutile as a new TiO$_2$-phase occurred. Peak intensities and positions were shifted. No loss of oxygen or vanadium was detected. The reaction involves the formation of a rutile solid solution containing VO$_x$ species. XPS studies showed an oxidation state of 4.75 for V in the rutile solid solution as compared to 4.65 in the shcherbinaite. A rutile solid solution once formed could not be re-transformed.

The rutile solid solution was first found at 525 °C < T < 550 °C for compositions of 3 mol% < V$_2$O$_5$ < 5 mol%. The phase field for rutile solid solutions extends to 10 mol% < V$_2$O$_5$ < 12.5 mol% at 675 °C. For very high V$_2$O$_5$ concentrations (95 mol% V$_2$O$_5$) a eutectic reaction was found at 631 °C. The DTA runs showed a widened endothermic melting peak and a very sharp crystallization peak on cooling. A shcherbinaite structure remained with shifted peak intensities and positions due to the alloying of Ti-ions.

SEM inspections showed that the rutile formation and the eutectic reaction both cause a substantial grain growth and a loss of surface area. The catalytic activity is entirely lost when the rutile formation occurs. The knowledge of phase relations helps to find the appropriate processing conditions and to understand the aging phenomena of catalysts.

1. Introduction

Commonly used catalysts in industry are composed of highly dispersed particles of precious metals or transition metal oxides on oxide supports.[1] Both the particle size and the form of connection between the support and the active compound have a strong influence on the activity and selectivity of the catalysts.[2,3]

The tailoring of catalysts with defined properties requires deep fundamental knowledge about their operation and aging or deactivation which can only be obtained reliably when the catalysts are monitored under operating conditions. The catalyst may decay in many ways.[4–15] The principle effects of deactivation of catalysts are mainly caused by deposition, sintering, contamination or decomposition. Nevertheless, these can be grouped basically into five intrinsic mechanisms of catalyst decay: (1) poisoning, (2) fouling, (3) thermal degradation, (4) loss of catalytic phases by vapour compound formation accompanied by transport and (5) attrition. (1) and (4) are chemical in nature, whereas (2) and (5) are mechanical. There has been reported numerous applications of the TiO$_2$–V$_2$O$_5$ system.[16–22] Phase reaction was investigated by Bond et al.[20] who found rutile formation under feed gas conditions associated with a loss of oxygen and a predominantly four valent V-ion. The change of the metastable anatase to rutile is the subject of the work of Pask who found that contaminants reduce the transformation temperature.[23]

---

* Corresponding author. Tel.: +49 30 314 249 76; fax: +49 30 314 240 72.
E-mail address: habel@ms.tu-berlin.de (D. Habel).

This work is focussed on the phase development during catalyst processing under oxidising conditions. The oxidative dehydrogenation of propane (ODP) was selected as a praxis-relevant model reaction for the evaluation of the catalytic properties of the catalysts thus treated. The resulting XRD spectra were qualitatively used to construct a preliminary phase diagram. The measurements were completed by DTA and SEM investigations.

2. Experimental

2.1. Sample preparation for phase analysis

A pure commercial TiO_2-powder in the anatase modification with an average particle size of 100 nm was supplied by KRONOS International INC (KRONOS 1002). The impurities are mainly P_2O_5, K_2O and sulfate in the range >40 ppm. The active component V_2O_5 occurred in the shcherbinaite modification (Gfe Environmental Technology Ltd.). The specimens were homogenised by ball milling in cyclohexane for 1 h and subsequently dried in air at 100 °C. The annealing of the resulting powder was carried out in a MgO-stabilised zirconia (PSZ) crucible in an air chamber furnace (Nabertherm). The heating rate was 5 K/min and the final temperature (400–700 °C) was held for 4 h. For comparison, additional annealing cycles were done for 10 h to investigate the time behaviour.

2.2. Phase analysis

The phase content of the annealed powders has been investigated by X-ray-powder diffraction. A θ-θ-diffractometer with Cu Kα radiation was used (BRUKER AXS, D5005, variable divergence slits, position sensitive detector or scintillation counter). The phase analysis was carried out using the Diffrac-Plus/Search program.

For higher precision of the lattice parameter, Guinier patterns (ENRAF NONIUS FR 552, quartz (1 0 1 0) Johansson monchromator, AGFA Structurix D7 DW X-ray film) were taken which enabled the use of monochromatic radiation and an internal Si-standard. The data were processed by the least square fit program PULVER[24] in order to gain lattice parameters.

2.3. Thermal analysis and morphology

Thermal analysis was needed to inspect weight loss and reaction temperatures. In order to avoid reactions a MgO-stabilised ZrO_2 crucible was used. For weight loss measurements, specimens were annealed in a chamber furnace (4 and 10 h). The transformation temperature for faster reactions was determined by a DTA run (Netzsch STA 429).

The morphology of the catalyst materials was inspected by SEM (Philips XL 20) and an EDX detector for cation analysis (EDAX with UTW detector).

2.4. XPS studies

The measurements were carried out using a modified LHS/SPECS EA200 MCD system equipped with a Mg Kα source (1253.6 eV, 168 W). Spectra were run with a pass energy of 48 eV. The binding energy scale of the system was calibrated using Au $4f_{7/2} = 84.0$ eV and Cu $2p_{3/2} = 932.67$ eV from foil samples. The powder samples were mounted on a stainless steel sample holder. The base pressure of the ultra-high vacuum (UHV) chamber was 1×10^{-10} mbar. The position of the sample holder in the analysis chamber can be well reproduced allowing a good comparison of absolute intensities of different samples. Charging of the samples was taken into account by using the identical O 1s binding energy of 529.9 eV for TiO_2 and V_2O_5.[25,26] To correct for charging the O 1s core level peak maxima of samples heat treated at 500 and 675 °C were shifted by 3.5 and 2.4 eV, respectively. A Shirley background was subtracted from all spectra before peak fitting with a 30/70 Gauss-Lorentz product function was performed. Atomic ratios were determined from the integral intensities of the signals which were corrected using empirically derived sensitivity factors.[27]

2.5. Catalytic testing

The support TiO_2-powder KRONOS 1002 was mixed with 4 mol% V_2O_5 powder in a vibrating unit and heat treated at 500, 600 and 800 °C in air for 4 h. The heating rate was 5 K/min. During the heat treatment the V_2O_5 spread on the surface of the TiO_2.

The oxidative dehydrogenation of propane to propene (ODP) was used as test reaction. Before testing, the catalyst material was uniaxially pressed at 10–20 MPa. For the catalytic experiments a fixed-bed reactor (Ø = 6 or 12 mm) made of quartz, operated at ambient pressure and equipped with on-line gas chromatography was used. A reaction mixture consisting of 40 vol.% C_3H_8, 20 vol.% O_2 and 40 vol.% N_2 was passed through the undiluted catalyst (0.2–1 g; $d = 250$–355 μm) packed between two layers of quartz of the same particle size. Total flow rates from 10 to 150 cm^3/min were used depending on the type of catalyst.

3. Results and discussion

3.1. X-ray phase analysis

The samples can be identified in the following way: sample T99.5/V0.5/400/4:

T99.5 = 99.5 mol% of TiO_2
V0.5 = 0.5 mol% V_2O_5
400 = calcination temperature (°C)
4 = calcination time (h)

Table 1 shows the starting composition and the qualitative phase content as found by XRD. The phase content was calculated from a simple analysis of the peak height using

$$X_{\text{phase}} = \frac{I_{\text{phase}}}{SI_{\text{all phases}}}$$

Since the V-content is comparably small this simplification does not produce too large errors.

Table 1
Weight loss and XRD-results of various sample compositions in the system TiO_2–V_2O_5

Sample	Nr. in Fig. 2, Table 2	Weight loss (wt.%)	Anatase S-Q (wt.%)	Rutile S-Q (wt.%)	Shcherbinaite S-Q (wt.%)
T99.5/V0.5/400/4		0.16	100	0	0
T99.5/V0.5/450/4		0.15	100	0	0
T99.5/V0.5/500/4		0.12	100	0	0
T99.5/V0.5/500/10		0.36	100	0	0
T99.5/V0.5/550/4		0.29	100	0	0
T99.5/V0.5/600/4		0.27	100	0	0
T99/V1/400/4		0.06	100	0	0
T99/V1/450/4		0.12	100	0	0
T99/V1/500/4		0.13	100	0	0
T99/V1/500/10		0.39	98	0	2
T99/V1/550/4		0.35	99	1	0
T99/V1/600/4		0.25	95	5	0
T97/V3/400/4		0.08	91	0	9
T97/V3/450/4		0.12	91	0	9
T97/V3/500/4		0.15	91	0	9
T97/V3/500/10		0.45	89	2	9
T97/V3/525/10	3	0.12	94	0	6
T97/V3/550/4		0.21	90	3	7
T97/V3/600/4		0.69	21	80 (ss)	0
T97/V3/625/4		0.68	24	76 (ss)	0
T97/V3/650/4		0.69	12	88 (ss)	0
T97/V3/675/4		0.68	6	94 (ss)	0
T97/V3/700/4		0.76	0	98 (ss)	2
T95/V5/450/4		0.26	86	0	14
T95/V5/500/4		0.27	82	0	19
T95/V5/500/10		0.42	87	0	13
T95/V5/525/10		0.11	91	0	9
T95/V5/550/4		0.30	86	2 (ss)	12
T95/V5/600/4		0.38	85	4 (ss)	11
T95/V5/625/4		0.82	0	100 (ss)	0
T95/V5/650/4		0.85	0	96 (ss)	4
T95/V5/675/4	4	0.85	0	96 (ss)	4
T95/V5/700/4		0.91	0	98 (ss)	2
T90/V10/450/4		0.16	79	0	21
T90/V10/500/4		0.22	86	0	14
T90/V10/500/10		0.30	82	0	19
T90/V10/525/10		0.14	84	0	16
T90/V10/550/4		0.25	85	1 (ss)	14
T90/V10/600/4		0.25	79	2 (ss)	20
T90/V10/625/4		0.62	28	59 (ss)	14
T90/V10/650/4		0.83	0	87 (ss)	13
T90/V10/675/4		0.95	0	94 (ss)	6
T90/V10/700/4		0.98	0	90 (ss)	10
T87.5/V12.5/675/4		1.00	0	89 (ss)	11 (mod. Liquid)
T85/V15/675/4		1.12	0	86 (ss)	15 (mod. Liquid)
T82.5/V17.5/675/4		0.93	0	80 (ss)	20 (mod. Liquid)
T80/V20/450/4		0.36	71	0	29
T80/V20/500/4		0.44	55	0	45
T80/V20/525/10		0.12	71	0	29
T80/V20/550/4		0.05	54	2 (ss)	45 (mod. Liquid)
T80/V20/600/4		0.20	60	2 (ss)	37 (mod. Liquid)
T80/V20/625/4		0.51	24	44 (ss)	33 (mod. Liquid)
T80/V20/650/4		0.68	0	69 (ss)	31 (mod. Liquid)
T80/V20/675/4	5	0.56	0	78 (ss)	22 (mod. Liquid)
T80/V20/700/4		0.86	0	77 (ss)	23 (mod. Liquid)
T50/V50/675/4		0.46	0	49 (ss)	52 (mod. Liquid)
T5/V95/675/4	6	0.39	0	0	100

Table 2
Measured and theoretical crystal data

Material	Sample in Table 1	Phases	a_0 (nm)	b_0 (nm)	c_0 (nm)
Reference materials					
ICPDS 21-1272		Anatase	3.785	–	9.514
ICPDS 21-1276		Rutile	4.593	–	2.959
ICPDS 41-1426		Shcherbinaite	11.516	3.566	4.373
Starting powders					
TiO_2	1	Anatase	3.785 ± 1		9.519 ± 2
TiO_2 annealed at 1200 °C	2	Rutile	4.593 ± 1		2.959 ± 1
V_2O_5	7	Shcherbinaite	11.519 ± 7	3.563 ± 2	4.370 ± 2
Catalyst specimens					
97 mol% TiO_2 / 3 mol% V_2O_5	3	Anatase	3.785 ± 1	–	9.515 ± 5
		Shcherbinaite	11.490 ± 1	3.564 ± 2	4.369 ± 2
95 mol% TiO_2 / 5 mol% V_2O_5	4	Rutile-(ss)	4.588 ± 1	–	2.958 ± 1
80 mol% TiO_2 / 20 mol% V_2O_5	5	Rutile-(ss)	4.586 ± 1	–	2.958 ± 1
		Shcherbinaite	11.519 ± 1	3.565 ± 3	4.369 ± 4
5 mol% TiO_2 / 95 mol% V_2O_5	6	Shcherbinaite	11.527 ± 7	3.567 ± 2	4.362 ± 4

Some of the phases showed variations with respect to peak position and height. Thus, in order to gain more accuracy the spectra were measured by a Guinier camera. The derived lattice parameters are given in Table 2.

The phase relations are discussed for increasing temperatures.

25–525 °C: For temperatures up to 525 °C the mixed V_2O_5/TiO_2 pattern showed the reflexes of anatase beside shcherbinaite. Their lattice parameters are very close to the reference data (samples 1 and 2 in Table 2). There was no indication for further phases. Thus, one can conclude that no alloying has taken place. The contact between anatase and shcherbinaite could have only been formed during heat treatment most probably due to surface diffusion of the vanadium species.

525–700 °C: For increasing temperatures, formation of rutile was found starting at about 550 °C which is significantly lower than for pure TiO_2. The literature mentions some results for the formation of rutile in the presence of various contaminants.[23] In this work, the transformation from anatase to rutile was encouraged by the presence of V_2O_5. In contrast, pure TiO_2 powders require temperatures of 900–1000 °C for the transformation. The V_2O_5/TiO_2 catalysts transformed to the rutile structure already at temperatures beneath 600 °C. The peak intensities are modified and the lattice parameters are shifted to smaller values (cf. Table 2). This indicates the formation of a rutile solid solution (henceforth denoted as rutile-(ss)) in which the V_2O_5 is dissolved.

In order to investigate the extension of the field of rutile-(ss), a series of samples with compositions from 0 up to 20 mol% V_2O_5 has been annealed at 675 °C. The specimens with 3, 5 and 10 mol% V_2O_5 content exhibited only the reflexes of the rutile-(ss). For 12.5 mol% and higher concentrations, an additional shcherbinaite phase with modified peak positions was detected (cf. Table 2, sample 5). Thus, the phase field of the rutile-(ss)

begins at 3–5 mol% V_2O_5 and 525–550 °C and extends to more than 10 mol% V_2O_5 at 675 °C.

The formation of a rutile-(ss) may be regarded as a solid state reaction:

$$TiO_2 \text{ (anatase)} + V_2O_5 \text{ (shcherbinaite)}$$
$$\Rightarrow Ti_{1-x}V_xO_y \text{ (rutile-(ss))}$$
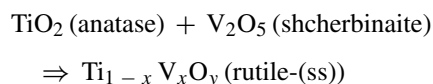
This reaction was first observed under the conditions:

$$525\,°C < T < 550\,°C \text{ for } 3 \text{ mol% } V_2O_5 < x < 5 \text{ mol% } V_2O_5$$

This type of reaction could formally be a eutectoidal type reaction which, however, would cause an endothermic signal on heating. A second possibility is a reaction from metastable starting phases to thermodynamically stable product phases which would cause a (sluggish) exothermic reaction. The DTA run on 10% V_2O_5 powder mixtures did not show any exothermic effect, the signal was very small, but the samples did react to rutile-(ss) and changed their colour. Thus, simple eutectic reaction can be excluded. A rutile-(ss) once formed at elevated temperatures could not be re-transformed to anatase. This proves that the rutile formation has to be seen as a reaction to form a thermodynamically stable product. The phase fields in the low temperature area have to be seen as metastable fields. The rutile-(ss) field will extend down to room temperature in a stability phase diagram. For practical purposes, however, the metastable phase relations are of more importance.

Eutectic reaction: For temperatures above 625 °C, rutile-(ss) and a vanadium rich melt are co-existing. A eutectic melt was already mentioned in ref.[28], however, the publication presented only a melt projection showing a eutectic reaction in the V_2O_5-rich regime.

Differential thermal analysis of a 5 mol% TiO_2–95 mol% V_2O_5 specimen showed a hysteresis for heating and cooling cycles and a sharp peak for the eutectic temperature at 631 °C
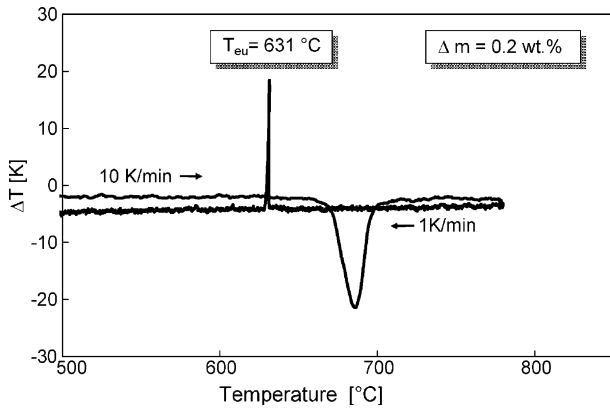
Fig. 1. DTA-plot of 95 mol% V_2O_5/5 mol% TiO_2.

Fig. 3. XRD-plot of a pure rutile and the rutile-(ss).

(cf. Fig. 1), which is taken as the eutectic temperature of this system.

The V_2O_5–TiO_2-melt forms on heating. The DTA plot shows a sharp crystallisation peak on cooling. The resulting TiO_2-containing V_2O_5-(ss) shows the crystallography of the shcherbinaite, however, with different lattice parameters. This is a result of the alloying of Ti-ions into V_2O_5 on melting.

3.2. Preliminary phase diagram

Based on the XRD results a working phase diagram was deduced (Fig. 2). The numbers 1–7 are the numbers of specimens corresponding to those in Table 2.

The straight lines indicate the stable equilibria, while the dotted lines show the metastable diagram for the given conditions. A continuous melt regime, a eutectic reaction and an extended rutile-(ss) belong to the stable part. The anatase–shcherbinaite miscibility field below 550 °C has to be considered as a metastable situation.

3.2.1. Rutile solid solution

Fig. 3 shows the comparison of the peak position of a pure rutile and that of a rutile-(ss) formed by a 95 mol%
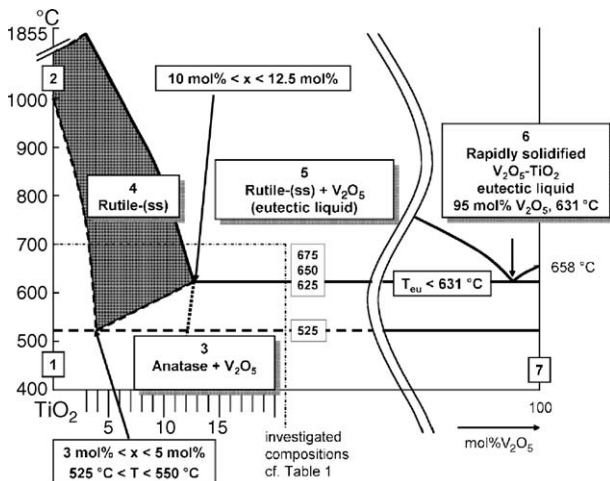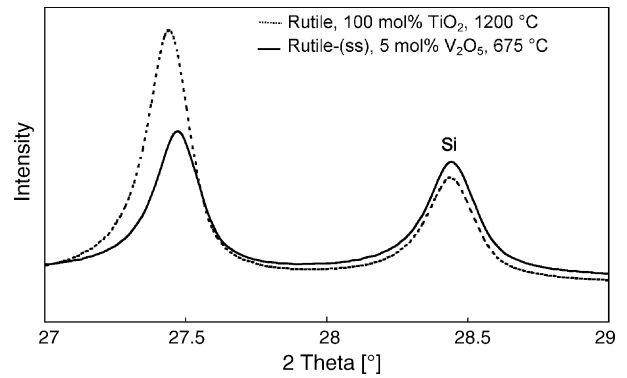

Fig. 2. Preliminary phase diagram of the system TiO_2–V_2O_5 under oxidising conditions.

TiO_2–5 mol% V_2O_5 mixture at an annealing temperature of 675 °C.

The unit cell of the rutile-(ss) is smaller than that of the pure rutile. Since V-ions both in the 4 and 5 valent state are smaller than Ti-ions, this behaviour indicates a substitutional replacement.

For this rutile-(ss) different defect models may be considered:

(1) Vanadium remains entirely in the 5 valent state; no loss of oxygen occurs; charge compensation by interstitial oxygen ions:

$$V_2O_5 \underset{TiO_2}{\Rightarrow} 2V_{Ti}^{\bullet} + O_i'' + 4O_O^x$$
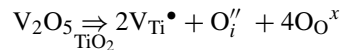
(2) Vanadium remains entirely in the 5 valent state; no loss of oxygen occurs; charge compensation by vacancies on the vanadium site:

$$2V_2O_5 \underset{TiO_2}{\Rightarrow} 4V_{Ti}^{\bullet} + Vac_{Ti}'''' + 10O_O^x$$
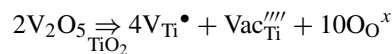
(3) Vanadium is reduced to the 4 valent state with loss of ½ O_2:

$$V_2O_5 \underset{TiO_2}{\Rightarrow} 2V_{Ti}^x + 4O_O^x + \frac{1}{2}O_2(v) \uparrow$$
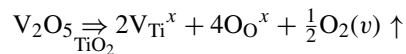
This type of solid solution has been described by Bond and Sarkany,[16] but those specimens have been annealed under reducing conditions. Hence, a significant weight loss was reported which is due to the evaporation of oxygen (MS spectra). The major difference in this work is the use of the atmosphere during thermal treatment. Because V_2O_5 is known to have high vapor pressure[29] the risk of evaporation had to be taken into account. If one assumes an evaporation of oxygen a significant weight loss should be observable. For the type (3) reaction the weight loss should be 1.8 wt.% for 10 mol% V_2O_5 and 3.2 wt.% for 20 mol% V_2O_5. However, the weight loss after annealing at different temperatures was ranging from 0.1 to 1 wt.% only (cf. Table 1). There was no indication for an influence of the V_2O_5 concentration on the weight loss but one for time and temperature. Additional ICP-OES investigations of the V-content showed that no significant change of the chemical composition could be recognised. Thus, a type (3) defect model is unlikely
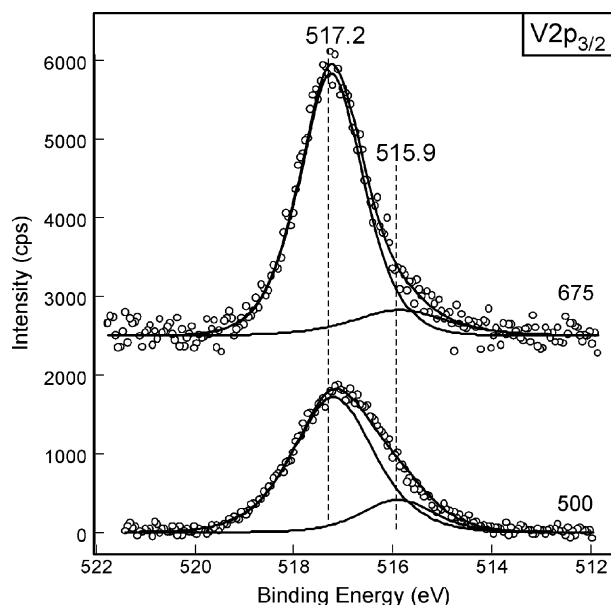
Fig. 4. V $2p_{3/2}$ spectra of 10 mol% V_2O_5/90 mol% TiO_2 heat treated at various temperatures.

Fig. 5. SEM-image of 5 mol% V_2O_5/95 mol% TiO_2 annealed at 550 °C.

for oxidising conditions; V cannot be entirely reduced to its 4 valent state.

On the other hand, a change of the colour of the samples was recognised. The V_2O_5/TiO_2 starting mixture is white or yellow whereas the reacted rutile-(ss) is brown-grey. The darkness of the colour increases with increasing V_2O_5 content and could be explained by a partly filled conduction band and metallic bonding character.

XPS studies were needed to determine the changes in oxidation state of V during temperature treatment. Fig. 4 shows V $2p_{3/2}$ spectra of samples with 10 mol% V_2O_5 heat treated at different temperatures (T90/V10/500/4 and T90/V10/675/4).

The peak can be described as the sum of two components centered at 517.2 eV (A) and 515.9 eV (B). The position of component A agrees well with the V $2p_{3/2}$ binding energy we have observed for V_2O_5, in which vanadium is expected to be in its highest oxidation state (+5). Therefore, we attribute component A to the V^{5+} oxidation state. As the *absolute* values of the binding energies of vanadium in all oxidation states vary significantly in the literature, the assignment of component B was based on the reported *differences* in the binding energies, ΔBE, of V^{5+} and lower oxidation states. Generally, the reported ΔBE between V^{5+} and V^{4+} is 0.7–1.0 eV and the reported ΔBE between V^{5+}
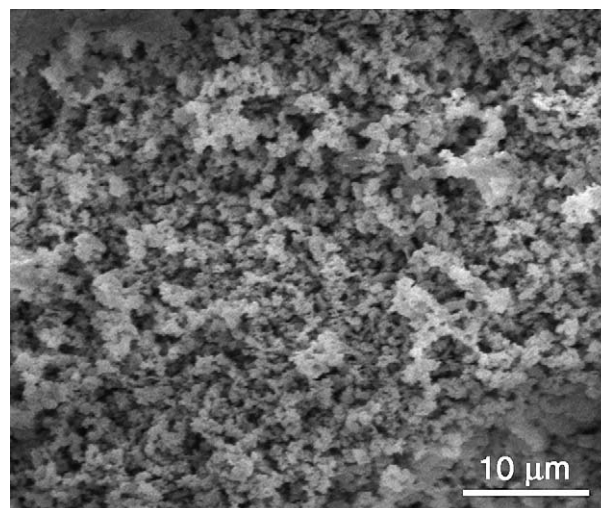
and V^{3+} is 1.2–1.5 eV.[30] This suggests that component B corresponds to the V^{3+} oxidation state.

Based on the spectral weight of the corresponding V^{5+} and V^{3+} states, the oxidation states of the samples T90/V10/500/4 and T90/V10/675/4 are calculated as 4.65 ± 0.07 and 4.75 ± 0.03, respectively. This means that both samples contain a mixture of vanadia in the 5 valent state and in the 3 valent state. The performed XPS analysis leads to the conclusion that the oxidation state of the sample heat treated at 500 and 675 °C is the same for both samples within the experimental error.

3.3. Phase morphology

At temperatures under 550 °C the initial phases anatase and shcherbinaite remain stable and the contact can be only formed via surface diffusion. A material prepared in this regime is characterized by fine and homogenous particles, cf. Fig. 5. This phase composition gives the best catalytic behaviour of the system in the ODP (Table 3).

For temperatures between 550 and 631 °C a eutectoid solid state reaction takes place and rutile-(ss) occurs.

If a TiO_2 supported catalyst is being exposed to high temperatures a substantial grain growth is observed (cf. Fig. 6). Since the reaction starts from the two pure phases the reaction path has to cross the stability field of the melt, which is expected to have much faster transport mechanism. The formation of a rutile at

Table 3
Catalytic results of the ODP at 500 °C of samples calcined at different temperatures under study (40 vol.% C_3H_8, 20 vol.% O_2, 40 vol.% N_2, contact time $\tau = 0.75$ g s/ml)

Catalyst	Calcination temperature (°C)	X C_3H_8 (%)	Y C_3H_6 (%)	S C_3H_6 (%)	S CO (%)	S CO_2 (%)	S C_2H_6 (%)	S Oxyg (%)
KRONOS-TiO2/V2O5 spreaded	500	20.1	7.7	38.3	34.0	22.9	4.8	<0.1
	600	18.4	7.2	39.0	35.6	22.6	2.8	<0.1
	800	<0.1	<0.1	<0.1	<0.1	<0.1	<0.1	<0.1

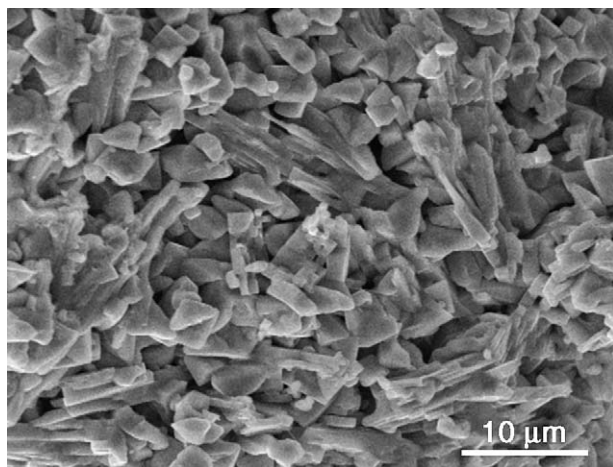Propane conversion (X), product selectivity (S) and propene yield (Y).

Fig. 6. SEM-image of 10 mol% V_2O_5/90 mol% TiO_2 annealed at 675 °C.

temperatures higher than the eutectic temperature will proceed via a solution (V_2O_5-rich melt) and a re-precipitation (TiO_2-rich solid). The catalytic activity of this material is almost zero (cf. Table 3).

For high V_2O_5-concentrations and temperatures above the eutectic temperature a liquid phase enhances the reaction rate as can be seen in Fig. 7. Very large clearly facetted grains were formed. The EDX spectra show that these particles still contain the full amount of V_2O_5. The morphology is needle like which corresponds well with the orthorhombic structure of shcherbinaite.

3.4. Catalytic activity

The calcination temperature exerts a large influence on the catalytic activity in the ODP reaction (cf. Table 3).

Only the material prepared at low temperatures (<550 °C, cf. Fig. 5) exhibits acceptable catalytic behaviour, i.e. these phases are catalytically active but metastable. As soon as the reaction to rutile-(ss) occurs the catalytic activity collapses (cf. Fig. 6). The active phase is no longer in contact to the gas phase and further the surface area is substantially decreased.
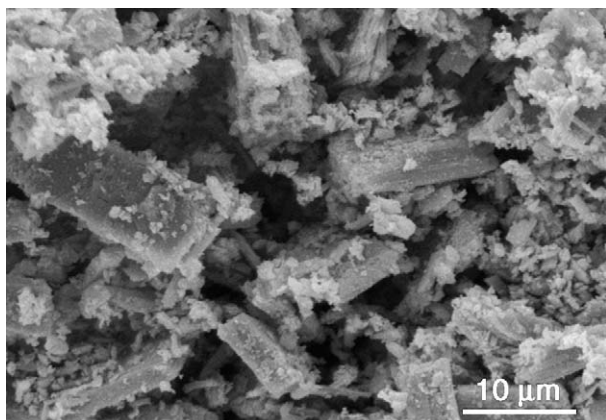

Fig. 7. SEM-image of 95 mol% V_2O_5/5 mol% TiO_2 annealed at 675 °C.

Detailed studies on the catalytic activity and its correlation with morphology and phase content is depicted in.[22]

4. Conclusion and outlook

The phase development in the system consisting of TiO_2 (anatase) and V_2O_5 (shcherbinaite) was investigated with TiO_2–V_2O_5 specimens prepared by ball milling and annealing in air from 400 to 700 °C. The XRD-results showed the formation of a rutile-(ss). Investigations of the SEM-EDX and ICP-OES underlined that the rutile being formed is a TiO_2–V_2O_5 solid solution.

A working phase diagram was deduced. For the temperature range up to 525 °C only anatase beside shcherbinaite is found for all compositions. This indicates a wide solubility gap. For higher temperatures, a metastable rutile solid solution field extends up to about 12.5 mol% V_2O_5. Until now it is not clear which defect model applies for this rutile solid solution. The reaction from anatase and shcherbinaite to the rutile-(ss) begins at 3 mol% < V_2O_5 < 5 mol% and 525 °C < T < 550 °C. The reaction is considered as a sluggish reaction from metastable to stable phases.

For high V_2O_5 concentration a eutectic reaction was recognised at 631 °C. For higher temperatures the reaction from anatase to rutile might proceed via a liquid phase which results in a substantial growth of the initial 100 nm anatase particles to form the final rutile grains of 1 μm in size.

V_2O_5/TiO_2 catalysts calcined at T > 600 °C show no catalytic activity since there is no accessible VO_x phase due to the solid solution of V_2O_5 in rutile.

Acknowledgements

References

1. Ertl, G., Knözinger, H. and Weitkamp, J., *Preparation of solid catalysts*. Wiley-VCH, 1999.
2. Stelzer, J. B., Kosslick, H., Caro, J., Habel, D., Feike, E. and Schubert, H., *Chem. Ing. Tech.*, 2003, **7**, 872–877.
3. Stelzer, J. B., Pohl, M.-M., Kosslick, H., Caro, J., Habel, D., Feike, E. and Schubert, H., *Chem. Ing. Tech.*, 2003, **11**, 1656–1660.
4. Farranto, R. J. and Bartholomew, C. H., *Fundamentals of industrial catalytic processes*. Chapman & Hull, 1997.
5. Bartholomew, C. H., Agrawal, L. K. and Katzer, R., *Adv. Catal.*, 1982, **31**, 135–142.

6. Bartholomew, C. H., Baker, R. T. and Dadyburjor, D., In *Stability of supported catalysts: sintering and redispersion*, ed. J. A. Horsley. Catalytic Studies Division, 1991.

7. Fuentes, G. A., *Appl. Catal.*, 1985, **15**, 33–40.

8. Menon, P. G., *Chem. Rev.*, 1994, **94**, 1021–1046.

9. Rueckenstein, E. and Dadyburjor, D. B., *Chem. Eng.*, 1983, **3**, 251–257.

10. Trimm, D. L., *Appl. Catal.*, 1983, **5**, 263–290.

11. Beltramini, J. N., *Arabian J. Sci. Eng.*, 1996, **21**, 225.

12. Li, W. D., Chen, M. J., Wang, X. H., Lu, X. W., Li, Y. H., Cheng, J. S. *et al.*, *Stud. Surf. Sci. Catal.*, 1994, **88**, 617–624.

13. Englisch, M., Ranade, V. S. and Lercher, J. A., *Appl. Catal. A Gen.*, 1997, **163**, 111–122.

14. Best, D. A. and Wojciechowskie, B. W., *Can. J. Chem. Eng.*, 1976, **54**, 1976–1983.

15. Grzesik, M., Skrzypek, J. and Wojciechowskie, B. W., *Chem. Eng. Sci.*, 1992, **47**, 4049–4055.

16. Bond, G. C. and Sarkany, A. J., *J. Catal.*, 1979, **57**, 476–493.

17. Piechotta, M., Ebert, I. and Scheve, J., *Anorg. Allg. Chem.*, 1969, **368**, 10–17.

18. Bond, G. C., Zurita, J. P. and Flamerz, S., *Appl. Catal.*, 1986, **22**, 361–378.

19. Yoshida, S., Murikama, T. and Tarama, K., *Bull. Inst. Chem. Kyoto Univ.*, 1973, **51**, 195–201.

20. Bond, G. C. and Tahir, S. F., *Appl. Catal.*, 1991, **71**, 1–31.

21. Vejux, A. and Courtine, P., *J. Solid State Chem.*, 1978, **23**, 93–103.

22. Stelzer, J. B., Feldhoff, A., Caro, J., Fait, M., Habel, D., Feike, E. *et al.*, *Chem. Ing. Tech.*, 2004, **8**, 1086–1092.

23. Shanon, R. D. and Pask, J. A., *Am. Miner.*, 1964, **49**, 1707–1717.

24. Weber, Institute for Applied Geosciences, TU Berlin, 1988.

25. Moses, P. R., Wier, L. M., Lennox, J. C., Finklea, H. O., Lenhard, F. R. and Murray, R. U., *Anal. Chem.*, 1978, **50**, 579–585.

26. Kasperkiewics, J., Kovacich, J. A. and Lichtman, D., *J. Electron Spectrosc. Relat. Phenom.*, 1983, **32**, 123–132.

27. Briggs, D. and Seah, M. P., *Practical surface analysis*. Wiley, Chichester, 1990.

28. Solacolu, S. and Zaharescu, M., *Rev. Roum Chim.*, 1972, **17**, 1715–1724.

29. LaSalle, M. J. and Cobble, J. W., *J. Phys. Chem.*, 1955, **59**, 519–524.

30. Nag, N. K. and Massoth, F. E., *J. Catal.*, 1990, **124**, 127–132;
Colton, R. J., Guzman, A. M. and Rabalais, J. W., *Acc. Chem. Res.*, 1978, **11**, 170–176;
Sawatzky, G. A. and Post, D., *Phys. Rev. B*, 1979, **20**, 1546–1555;
Andersson, S. L. T., *J. Chem. Soc., Faraday Trans. 1*, 1979, **75**, 1356–1370;
Odriozola, J. A., Soria, J., Somorjai, G. A., Heinemann, H., Garcia de la Banda, J. F., Lopez Granados, M. and Conesa, J. C., *J. Phys. Chem.*, 1991, **95**, 240–246;
Eberhardt, M. A., Proctor, A., Houalla, M. and Hercules, D. M., *J. Catal.*, 1996, **160**, 27–34.